Chapter 2. Coordinate Systems and Data Displays

Plane wave front synthesis from reflection seismic data requires the introduction of a new set of coordinates. In this chapter we will investigate alternative self-consistent coordinate systems which describe the data when it is organized as a collection of plane wave fronts. Seismic sections generated by plane wave synthesis will show themselves to be similar in appearance to common midpoint sections.

Standard Coordinate Frames

The standard recording geometry of reflection seismology is shown in Figure 2.1. A single explosive source and many geophones (commonly 24 or 48) are arranged along a line on the earth's surface. The distance between contiguous geophone positions is constant. A single "experiment" is then performed which involves recording a seismogram at each geophone position immediately subsequent to discharging the source energy.

We shall define s to be the horizontal coordinate of the shot, and g to be the horizontal coordinate of the geophone. Two other descriptive coordinates can be introduced by the relations,

$$f = g - s \tag{2.1a}$$

$$y = \frac{s+g}{2} \tag{2.1b}$$

where f is the offset between a shot and a geophone position, and y is their midpoint.

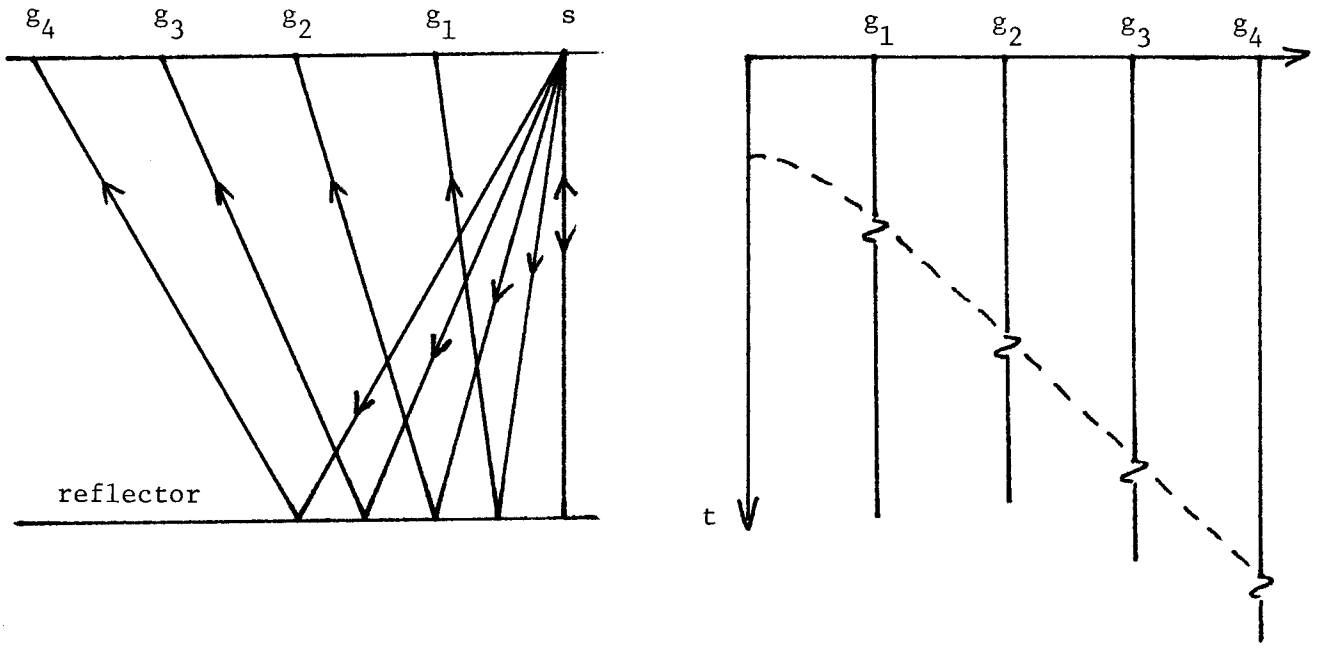

Figure 2.1. The geometry and data display for the common shot gather. The data display is the same as one would expect for the CMP geometry below as long as reflectors are flat.

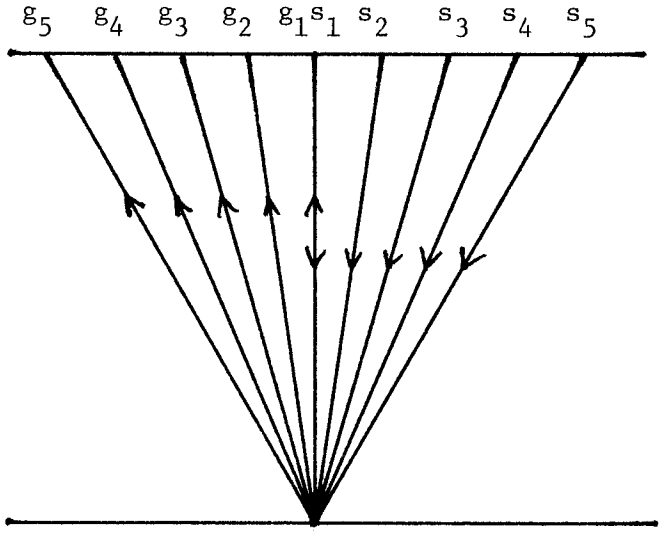

Figure 2.2. The common midpoint (CMP) geometry.

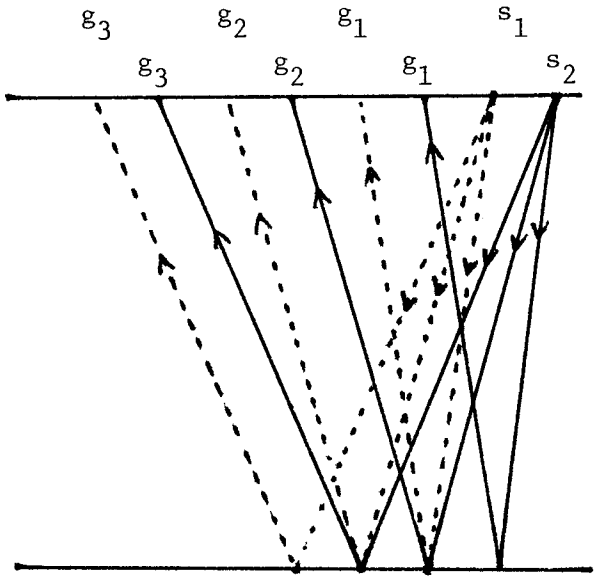

Figure 2.3. Geometry for two successive experiments showing data collection redundancy.

For the single reflector of Figure 2.1, the arrival times t of the reflected energy to the geophone positions is described by

$$t^2 = t_0^2 + \frac{f^2}{v^2} \tag{2.2}$$

where t_0 is the zero-offset travel time and v is the (constant) acoustic velocity. Equation (2.2) assumes that the reflector is horizontal. Dipping reflectors will be discussed in some detail in Chapter 4.

Note that equation (2.2) describes the travel time curve for both the geometry of Figure 2.1 with the shot coordinate s constant, and the geometry of Figure 2.2 with the midpoint coordinate y a constant. The data displays shown in Figures 2.1 and 2.2 are created by laying seismograms side by side with time increasing downward, and offset increasing to the right. They will be described as common shot and common midpoint (CMP) gathers respectively.

The geometry of Figure 2.2 with no other ray paths than those depicted cannot be realized from a single physical experiment. Rather, 5 individual experiments are required: shot s_1 must be fired with only geophone g_1 listening, then s_2 with only g_2, etc. This is achieved in the field by a high redundancy level using the geometry of Figure 2.1. Figure 2.3 shows how this is achieved by picturing two sequential field experiments. The ray paths from shot position s_1 are shown as solid lines. The entire experiment is then moved to the right by one-half the group interval and a second experiment is performed, resulting in the dashed ray paths. The process is continued in this manner creating seismograms of all offsets for any midpoint.

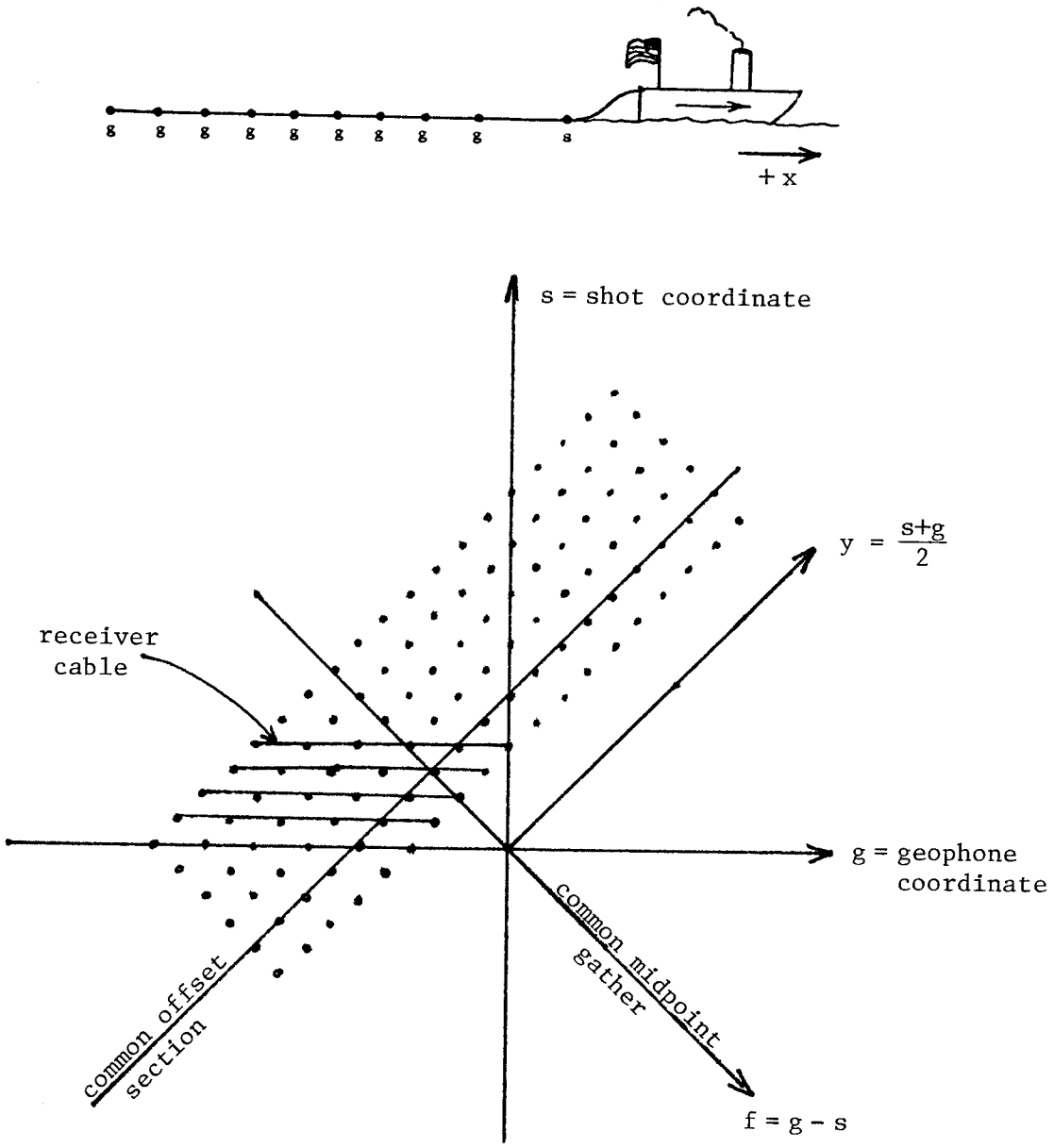

Figure 2.4. This diagram shows the relations among the horizontal coordinates y, f, s, and g. All axes are parallel to the path of the boat which moves in the $+x$ direction. The five parallel lines show the position of the receiver cable for five consecutive shots.

Each point represents a seismic trace. The display modes common midpoint gather and a common offset section are shown. The common shot (geophone) gather is data along a horizontal (vertical) slice.

A convenient way to display this "multi-fold" data is shown in Figure 2.4, with each dot representing a single seismogram.

The Slanted Plane Wave Stack

Consider a common geophone gather. This is seismic data in (f,t) coordinates for a constant geophone position, g. (This would be data along any line parallel to the s axis in Figure 2.4.) Let us now instead of visualizing a collection of ray paths from each shot to the geophone, visualize a spherical wave front diverging from each shot position.

Figure 2.5 shows the geometry for a possible single experiment which we could perform. If we placed a single geophone and an array of shots as shown in the figure, and then fired all shots simultaneously, we would be synthesizing a downgoing plane wave front by the superposition of many spherical wave fronts. (More properly, we should be discussing propagating cylindrical rather than plane wave fronts, but for the purposes of this thesis we have assumed the earth to be two-dimensional. Then, except for differing factors for amplitude decay due to geometrical spreading, the two will be equivalent. Since visualizing plane waves is easier than visualizing cylindrical ones, we will continue to speak of plane waves.)

The downgoing plane wave can also be synthesized by a superposition of many single shot-single geophone experiments. Let $P(f,t)$ be the data in (f,t) coordinates with g constant. We now perform the operation

$$P'(t) = \sum_{i=1}^{i=5} P(f_i, t) \qquad (2.3)$$

where we are summing over the offset coordinate to produce a single output trace, P'. This, by superposition, is equivalent to the

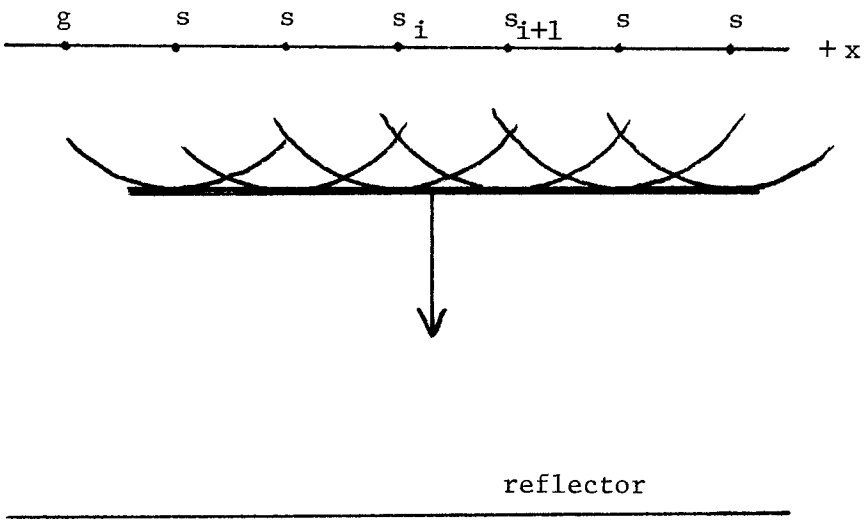

Figure 2.5. If we have a single geophone and many shots, we can imagine firing them all at the same time to create a downgoing plane wave in a single physical experiment. For a line source in 3-D, the wave front is actually cylindrical.

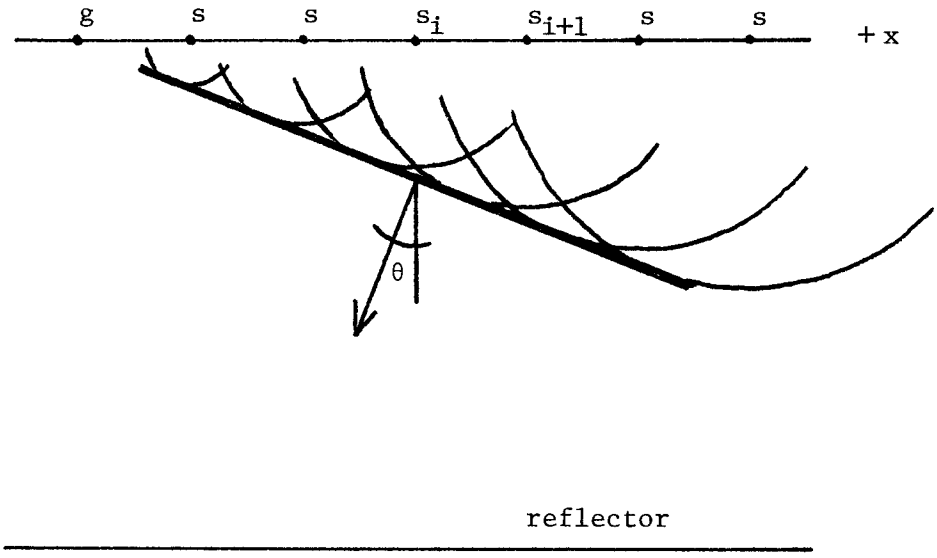

Figure 2.6. We can create a downgoing plane wave at some angle, θ, by firing the shots with time lags. For a line source in 3-D, the wave front is actually conical.

geophone recording of the single physical experiment shown in Figure 2.5.

An interesting generalization of the above is to synthesize a downgoing plane wave front propagating at some arbitrary angle, θ, to the horizontal.

Study of Figure 2.6 shows that the shot, s_i, must be fired with some time lag, δt, relative to shot s_{i+1}. If $\Delta s = s_{i+1} - s_i$, then

$$\delta t = -\frac{\Delta s}{v_H} = \frac{\Delta f}{v_H} \tag{2.4}$$

where v_H is the (constant in layered media) horizontal phase velocity of the propagating wave front, and is positive for a velocity in the $+x$ direction.

A relation well-known in seismology (see for example, Stacey, Chapter 4) is that for a vertically stratified earth,

$$p \equiv \frac{\sin\theta(z)}{v(z)} = \frac{1}{v_H} = \text{constant} \tag{2.5}$$

where p is commonly referred to as the ray parameter, $v(z)$ is the depth-dependent acoustic velocity of the medium, and θ and v_H are as defined above. The sign convention for p is such that p is positive when v_H is positive. Equation (2.5), true only in a vertically stratified velocity medium, states that the ray parameter thus defined is equal to the inverse of the horizontal phase velocity, and is independent of depth, z. Thus, it is an invariant property of the plane wave front as it propagates down into a layered earth.

Combining equations (2.4) and (2.5) we write,

$$\delta t = p\,\delta f \tag{2.6}$$

Now we are in a position to synthesize a downward propagating plane wave front with a particular ray parameter, p. We generalize equation (2.3) to

$$P'(p, t') = \sum_{i=1}^{n} P(f_i, t = t' + p f_i) \qquad (2.7)$$

Equation (2.7) gives us a transformation of data in (f,t) coordinates with g constant to data in (p, t') coordinates. The summation operation given by (2.7) will be referred to as a slant plane wave stack, or slant stack.

Equation (2.7) is valid for both positive and negative values of p for wave fronts traveling in the $+x$ and $-x$ direction respectively. By invoking reciprocity when necessary we can always have the wave front departing an array of shots and arriving at a single geophone. The following table shows the sign conventions for the case of a one-sided spread as in marine data.

	Boat moves in +x direction		Boat moves in -x direction	
	$p \geq 0$	$p \leq 0$	$p \geq 0$	$p \leq 0$
which gather?	common shot	common geophone	common geophone	common shot
invoke reciprocity?	yes	no	no	yes
sign of $f = g - s$	$f \geq 0$	$f \leq 0$	$f \geq 0$	$f \leq 0$

Note that equation (2.7) give us a method of synthesizing a wave front from individual shot-geophone experiments, and that these wave fronts will be planar only if the acoustic velocity is independent of the horizontal space coordinate (call it x). If, for example, we are dealing with marine data where the velocity structure below the sea-floor is very complicated, then what we have done is to create a downgoing plane wave front in the water, but some undulating wave front as it passes through the region below the sea floor. However, even in a case where the velocity is extremely laterally dependent we are still synthesizing propagating wave fronts, and although they may deviate from being planar, we shall be able to extrapolate them through space by methods based on approximations to the scalar wave equation (see for example, Claerbout and Johnson, 1971).

Because the scalar wave equation deals with propagating wave fronts, we must be able to create whatever data display with which we are dealing by a single physical experiment if we are to use the wave equation for any processing scheme. This is the reason that we have not included the common midpoint gather as an optional coordinate system over which to slant stack. There is no apparent way in which the common midpoint gather can be created by a single physical experiment, and therefore data created by slant stacking over the CMP gather likewise cannot be created by a single physical experiment.

Equation (2.2) and Figures 2.1 and 2.2 indicate that the trajectory of arrival times for a flat layer in a constant velocity medium as a function of offset will be a hyperbola. Figure 2.7 shows a common geophone gather from three reflectors. As indicated by equation (2.7), the summation trajectories for a slant stack with ray parameter p are straight lines with slope $\Delta t / \Delta f = p$. The dashed lines in Figure 2.7 show the three particular summation trajectories which are tangent to the hyperbolic events. These are the only occasions where we expect the slant sum to register a significant contribution from the events, because for a portion of the sum the phase will be coherent. This will be demonstrated, rather than proved, in the final section of this chapter and in Appendix A.

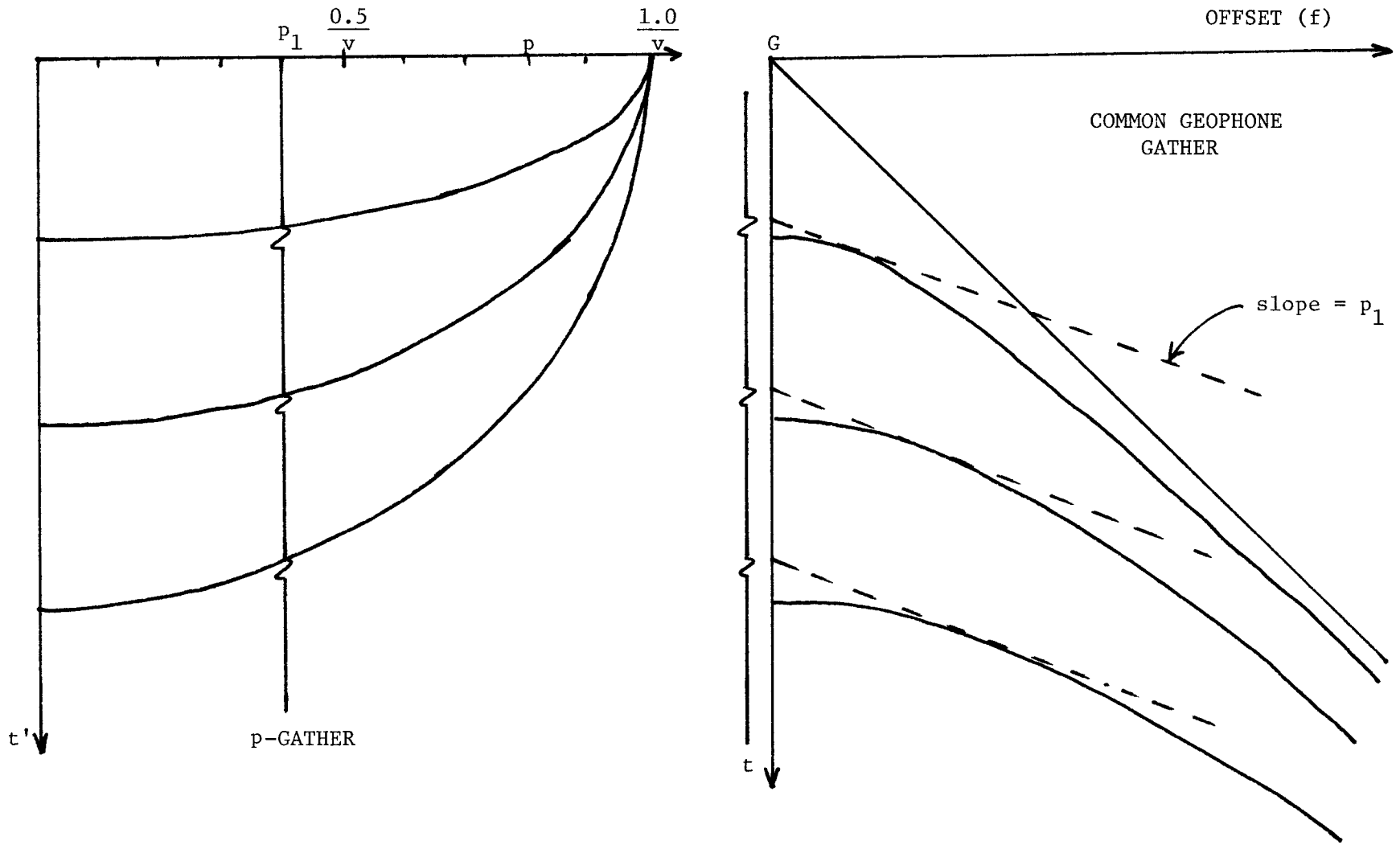

Figure 2.7. The slant plane wave stack transforms a common geophone (or shot) gather into a p-gather. To the right, in the common geophone gather, a sample slant stack is implied by the dashed lines showing the coherency summation. The output trace is shown. This trace is one of those comprising the p-gather, and is indicated in its proper position in the p-gather on the left.

The slant stack for this particular value of p will place the three events at locations on the time axis shown in the output trace. This resultant output trace will be one trace in our "p-gather", which is also shown in the figure. We shall show shortly that the slant stack transforms hyperbolic events into elliptical ones with a p axis intercept at $p = v^{-1}$, where v is the constant acoustic velocity.

A particularly instructive exercise is to investigate the slant stack for $p = 1/v$. In this case the dashed summation lines of Figure 2.7 will be parallel to the direct arrival, shown as the diagonal line from the origin. The direct arrival also marks the asymptote of all three hyperbolic events. For this value of p, the only summation trajectory for which we will obtain a stationary phase contribution will be the one which intercepts the origin, i.e., a summation trajectory coincident with the direct arrival event. In this case our value of t' will be equal to zero.

What we have just done was to create a plane wave with ray parameter equal to $1/v$, that is, a horizontally traveling wave from the shots toward the geophone. We have noted that in this case we get an arrival at $t' = 0$. This indicates that our t' coordinate, which we have identified with the slant plane waves, is equal to zero when the wave front intercepts the geophone position. This observation permits us to make use of the ray path diagram of Figure 2.8.

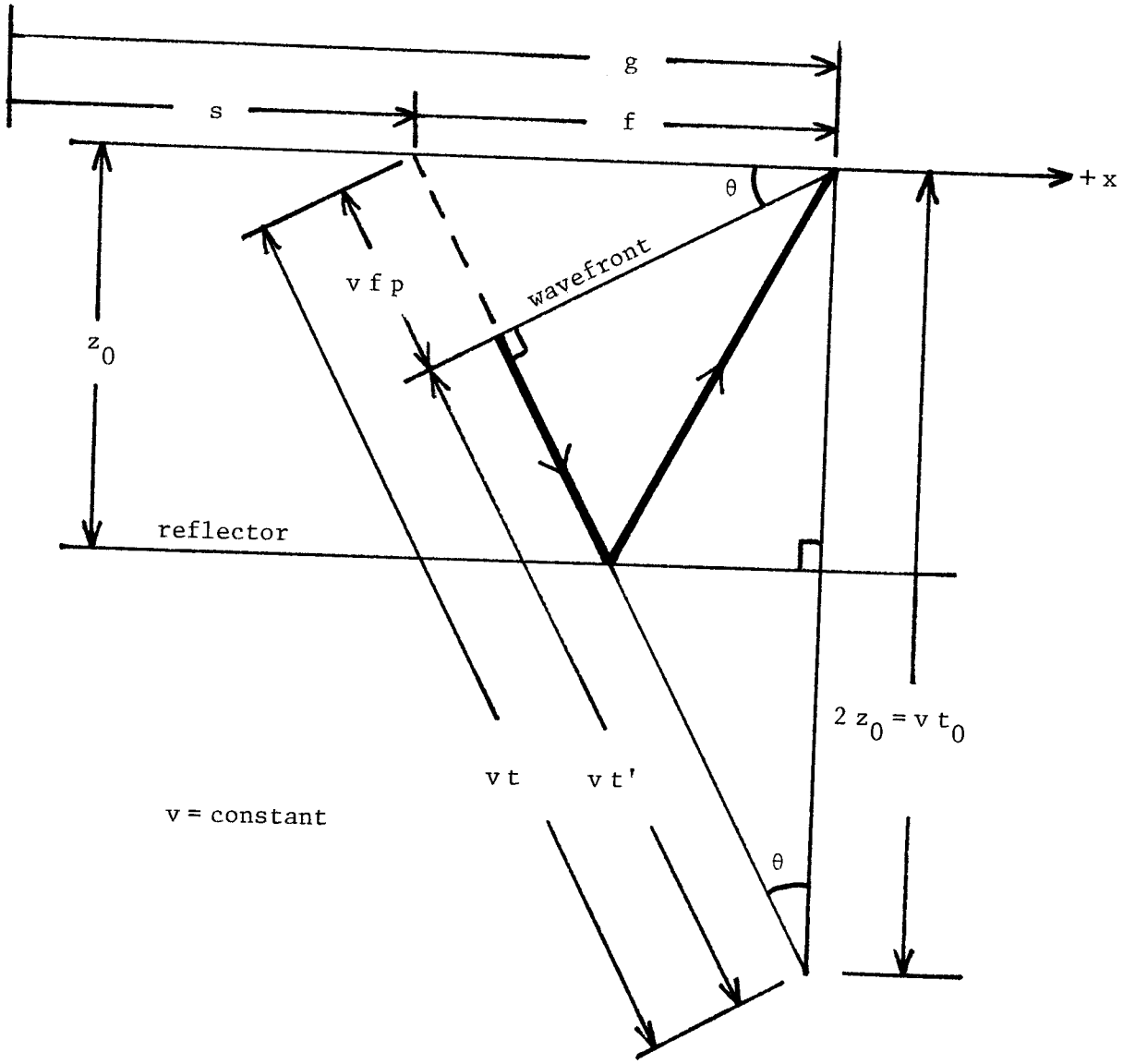

Figure 2.8. The slant frame geometry. The source is a downgoing plane wave front at angle θ to the horizontal, but for a geophone at position g, the reflected energy from z_0 emanates mainly from shot position, s. The slant frames require the introduction of a new time coordinate, $t' = t - f p$, where $p = \sin\theta(z) / v(z) =$ constant is the ray parameter.

The wavefront is propagating in the $+x$ direction, depicting the geometry for a positive value of p. Reciprocity has been invoked to reverse the roles of shot and geophone.

Figure 2.8 shows a snapshot of our propagating wave front at $t' = 0$. Also shown is the ray path which will be taken by the energy which will eventually reach the geophone position. Although we have a propagating wave front, most of the energy arriving at g will emanate from the shot position labeled s in the figure. Several interesting relations can be inferred here. If f is the offset between the geophone and the most important shot point, then the relation between the shot to geophone time, t , and the arrival time, t' , in the slant frame will be

$$t = t' + f p \tag{2.8}$$

The time difference, $f p$, between the shot-to-geophone time and the slant frame arrival time is equal to the time it takes for the horizontal phase velocity of the plane wave to travel from s to g . This is consistent with p being the inverse of the horizontal phase velocity.

If t_0 is the two-way vertical travel time to the reflector, then since our velocity, v , is constant, we have from the geometry of the figure,

$$\frac{t'}{t_0} = \cos\theta \tag{2.9a}$$

and

$$\frac{t_0}{t} = \cos\theta \tag{2.9b}$$

Incorporating equation (2.5) into (2.9) we have

$$\frac{t'^2}{t_0^2} + p^2 v^2 = 1 \qquad (2.10a)$$

and

$$\frac{t_0^2}{t^2} + p^2 v^2 = 1 \qquad (2.10b)$$

Equation (2.10a) describes an ellipse in (p, t') space. It verifies the form of the p-gather shown in Figure 2.7.

Figure 2.9 relates these various time coordinates in the original common geophone gather. It can be seen here that the coordinates f and t identified in Figure 2.8 relate to the offset and arrival time of that region of the hyperbolic event which is tangent to the slant summation trajectory. Thus, Figures 2.8 and 2.9 both show, but in different ways, that most of the important energy in the slant frame comes from the region around some individual shot.

Note that when a slant stack is done, nothing need be known but the ray parameter, p . Except for some practical problems discussed in Appendix A, there is no need for any velocity information prior to the stack. Equations (2.10) then can be used to estimate velocity the same way way equation (2.2) is used in the more standard geometries.

We emphasize at this point that the coordinates (x', p, t') are output directly from the slant stacking process. For example, in a stack over the common geophone gather in Figure 2.7, a single seismic trace is output. This trace has a fixed value of p (given by whatever the slope of the summation trajectory happens to be), and a fixed value of x' (given by the geophone coordinate, g). The time coordinate of the

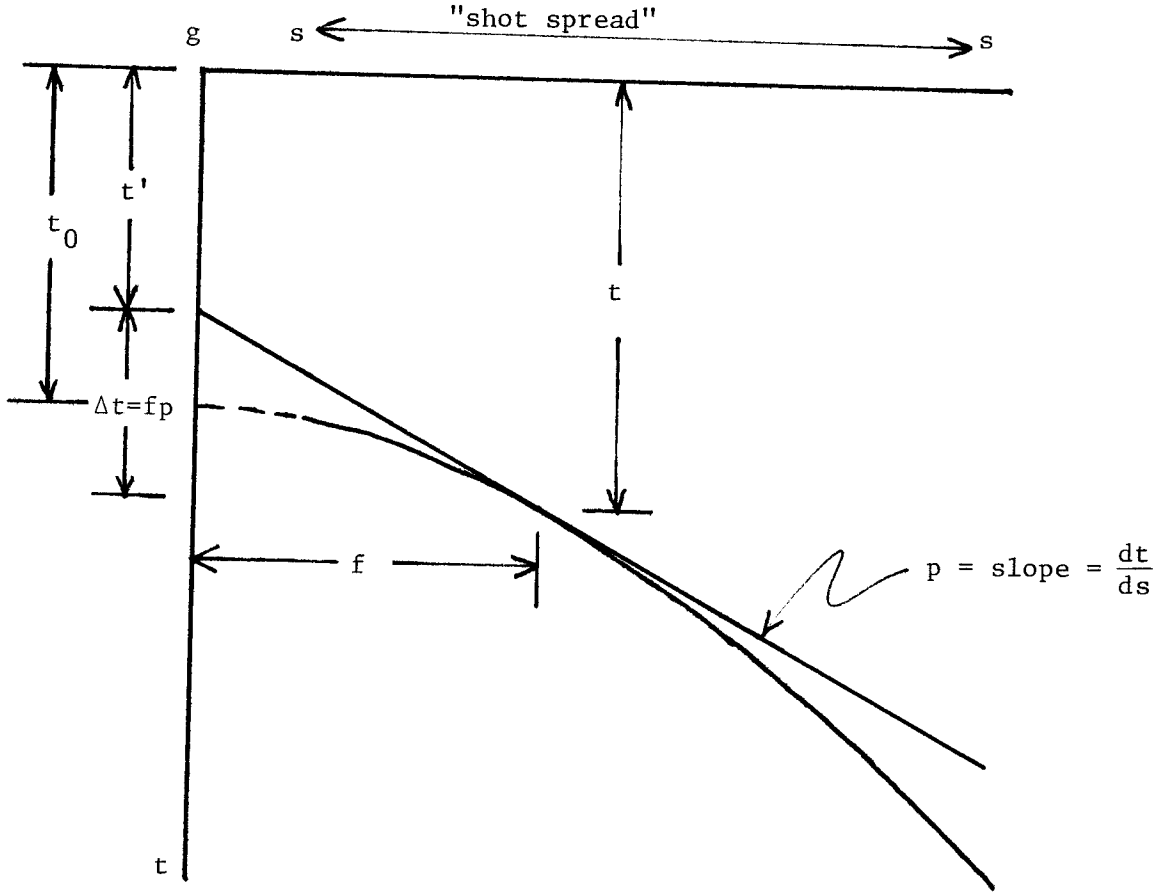

Figure 2.9. A single hyperbolic event shown in a common geophone gather. The line labeled "p" shows the stacking trajectory, and its intercept with the time axis defines t' for this particular event and stacking parameter p. The intervals marked f and Δt can also be seen on Figure 2.8 in real physical space. Figure 2.9 shows clearly the relationship $\Delta t = f p$, and also $t' = t - f p$.

output trace is defined to be t' . Thus, the simple operation of the slant stack transforms data from either (s, f, t) or (g, f, t) coordinates to (x', p, t') coordinates.

The Fresnel Zone

If the shot waveforms were perfect impulses, then the point of tangency of the slant sum trajectory with the hyperbolic event would indeed be a single point. In all practical cases the waveform is of finite duration and the dominant wave length will specify a region of tangency. The broad event of Figure 2.10 indicates the dominant period in the waveform, and shows the region of tangency. We shall call this region a Fresnel zone. Figure 2.11 shows the Fresnel zone for several events. How large is the Fresnel zone?

Figure 2.12 shows a propagation path from a single shot to a line of receivers. These receivers would actually be on the surface with s , but we have mirrored their position across a subsurface reflector. The maximum propagation distance for any frequency is Q wavelengths, where Q is the attenuation parameter. We shall assume that after this propagation distance, the energy has dropped so that we can no longer detect it.

We require that to be in the Fresnel zone, the maximum deviation in phase must be no greater than $\pm 2\pi / 3$ from the receiver shown in the centered position. A simple calculation shows that if we assign $Q = 100$ to the earth, the angular deviation, Ω , is about 9 or 10 degrees.

This is only a very crude calculation, but it serves to show that we should expect a data base reduction after the slant stack.

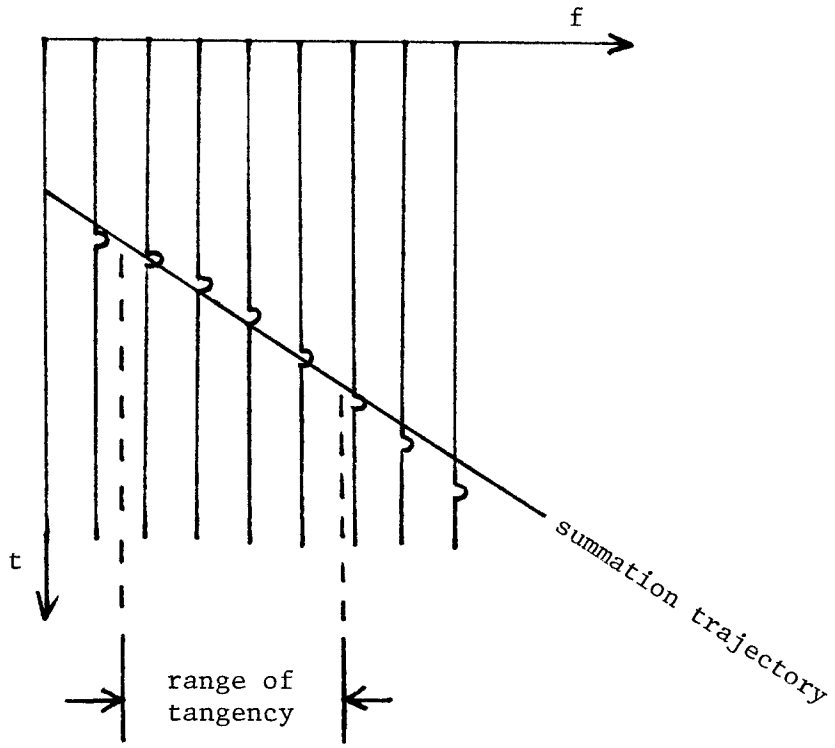

Figure 2.10. Because the waveform is of finite length, the tangency of the summation trajectory with the hyperbolic trajectory of the event will be larger than a geometrical point.

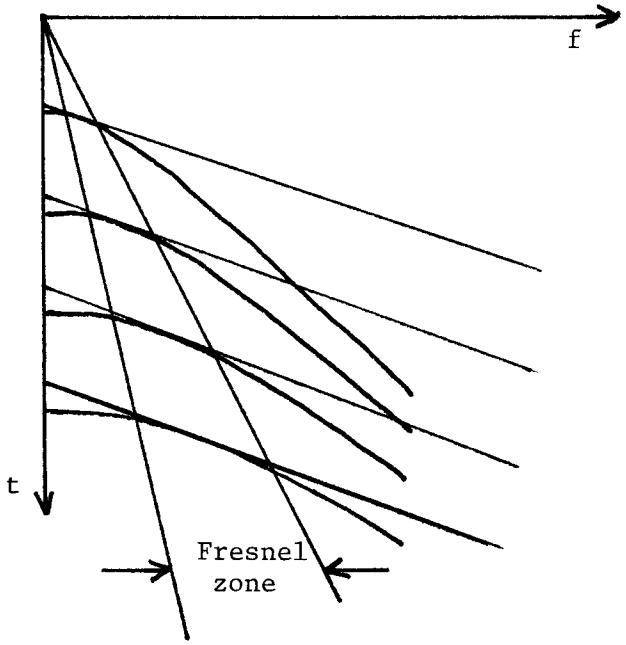

Figure 2.11. There will be a region, called a Fresnel zone, within which events and the summation trajectory will be tangent. The boundaries of the zone change as parameter p changes.

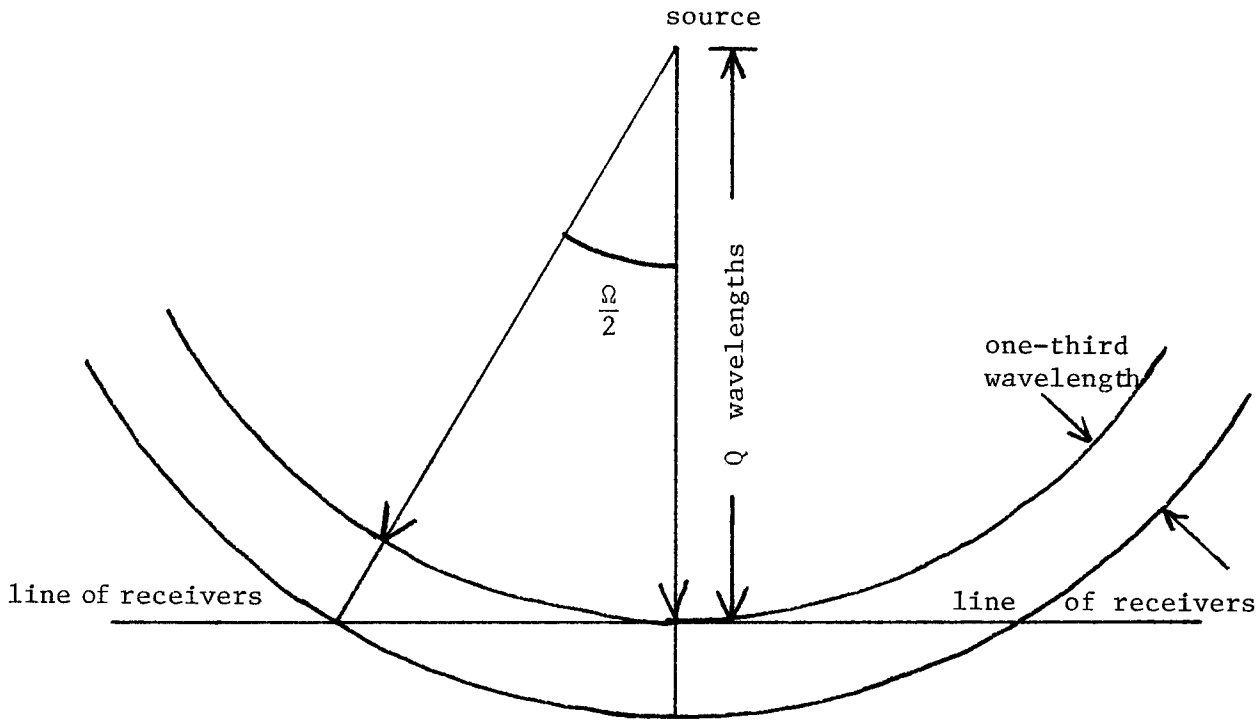

Figure 2.12. Our (arbitrary) definition of the Fresnel zone: Assume an earth with a finite value of Q, the attenuation parameter. Imagine a source of a signal with a dominant wavelength, and a line of receivers which are a distance Q wavelengths from the source. We define coherence such that the signals to the receivers must be within one-third period of being time coincident. With the help of the diagram, the angle, Ω, of the Fresnel zone is calculated for $Q = 100$.

$$\Omega = 2 \arccos\left(\frac{Q}{Q+3}\right) = 2 \arccos\left(\frac{100}{103}\right) \cong 9.5°$$

We can reasonably expect that we do not have a range of propagation angles in our data of more than 0 to 45 degrees, because of the finite geophone spread. If a single Fresnel zone encompasses approximately 10 degrees, we can speculate that 4 or 5 traces in the p-gather contain all the information in the original 24 or 48 trace common geophone (or common shot) gather.

This calculation ignores the effects of noise and other practical complicating factors, but it gives an optimistic result which we can modify subsequently. A 10 to 1 data compression is certainly too much to hope for, but the slant stack is a partial coherency stack and a very real data base reduction is expected. The next chapter compares velocity estimates in slant frames for several data compression factors.

Slant Plane Wave Interpretation Coordinates

Equation (2.7) indicate that we can transform recorded seismic data into the (p, t') slant frame beginning with either common shot or common geophone gathers. Rather than using the s or the g coordinate depending on the sign of p, we introduce the coordinate x', which specifies the geophone position when the slant stack is done over a common geophone gather, but the shot position when stacking over a common shot gather. The physical interpretation of x' is the surface position of a receiver picking up the reflected energy of the downgoing plane wave shown in Figure 2.8. The slant frame coordinates now become (x', p, t') with the sign of p positive when the plane wave front moves in the $+x$ direction.

Consider the data in the slant frame for some fixed value of p, say $p = p_0$. The data, $P'(x', p=p_0, t')$, can now be described as a "slant plane wave section", or "p-section." This data display would be the one of preference for geological interpretation, since it most

closely resembles a cross-section of the earth. Figure 2.13 shows a sample ray path for three flat reflectors in a constant velocity medium. A p-section with this particular angle, θ , would involve many traces with the same ray path geometry.

The geometry of Figure 2.13 involves all ray paths which contribute to the single trace at the surface position $x' = g$. The data trace unfortunately does not represent reflection points directly beneath the surface receiver position, x' . By definition, the coordinate x' is constant along the upcoming ray shown in the figure, and we would apparently like to define a new coordinate, x , which is constant for a fixed horizontal position in the earth. Thus, x would be an earth-based coordinate.

As seen clearly from the figure, we wish to do a uniform shearing of the data, the amount of which being dependent on the depth to the reflector of interest. As can be seen in the figure, this is true even in a constant velocity medium.

Let us write the relation

$$x = x' - \Delta x(z) \tag{2.11}$$

Now, if z is the depth to a reflector, and Δx is a horizontal dimension, we can immediately write, with the help of the simplified geometry of the constant velocity medium, that

$$\Delta x(z) = z \tan \theta \tag{2.12}$$

where $\theta = \arcsin(pv) = \text{constant}$. Note that in the figure p and Δx are negative.

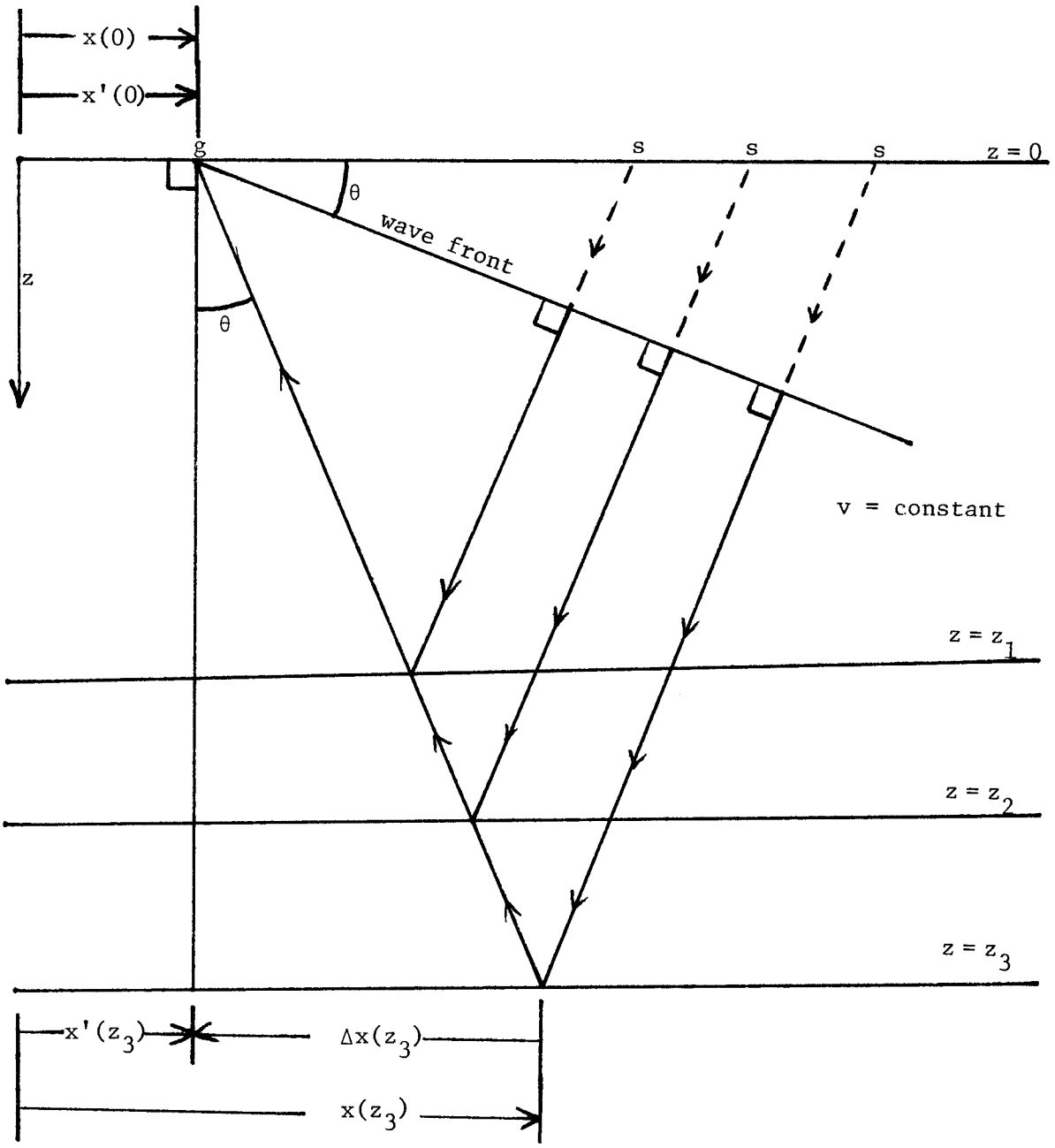

Figure 2.13. Ray paths in the slant frame for three horizontal reflectors in a constant velocity medium. Here the value of p is negative. The energy received at the geophone is displayed as a single trace by the slant stack process, but as seen in the figure really represents subsurface reflection points which lie along a ray path. Points along this ray path all have the same value of coordinate x'. Relations between x and x' are shown at depth $z = 0$ and $z = z_3$.

Recalling that t_0 is the vertical two-way travel time to a reflector at z, and re-expressing $\tan\theta$, we can rewrite (2.12).

$$\Delta x(t_0) = \left(\frac{v\,t_0}{2}\right) \frac{p\,v}{(1-p^2v^2)^{1/2}} \tag{2.13}$$

Now we have an expression, given by (2.13), for the amount of lateral shifting that we must do to the data as a function of the vertical travel time, t_0. This is not yet quite the desired situation, since the data in our p-section is in (x', t') coordinates, not (x', t_0). We must now combine equation (2.10a) with (2.13) to obtain

$$\Delta x(t', p, v) = \left(\frac{vt'}{2}\right) \frac{p\,v}{1-p^2v^2} \tag{2.14}$$

which is the desired result. Note that the transformation

$$x = x' - \frac{p\,v^2\,t'}{2(1-p^2v^2)} \tag{2.15}$$

can now be done directly in the slant frame coordinates. We observe also that we now require some input as to the true acoustic velocity.

Since the effort has just been made to derive a transformation of the horizontal slant frame coordinate, x', to an interpretation coordinate, x, it is certainly reasonable to make the same effort to transform t' into some other time coordinate more logical for display purposes. As it now stands, we have a time coordinate, t', which for a particular subsurface reflector has a different value for each unique p-section we create. A more reasonable time coordinate is t_0, the vertical two-way travel time. We have already determined the

transformation equation for t' to t_0, but we rewrite it here.

$$\frac{t'^2}{t_0^2} + p^2 v^2 = 1 \tag{2.10a}$$

or

$$t_0 = \frac{t'}{(1-p^2v^2)^{1/2}} \tag{2.16}$$

Equations (2.15) and (2.16) together define a transformation from (x', p, t') coordinates to what we shall call interpretation coordinates (x, p, t_0). We note again that the coordinates (x', p, t') come directly from the slant stacking process.

When the depth-dependent velocity is known only approximately (as is often the case), the transformation itself can be done only approximately. If $\hat{v}$ is the velocity estimate, then the transformation can be written

$$\hat{x} = x' - \frac{p\hat{v}^2 t'}{2(1-p^2\hat{v}^2)} \tag{2.15'}$$

and

$$\hat{t}_0 = \frac{t'}{(1-p^2\hat{v}^2)^{1/2}} \tag{2.16'}$$

The coordinates $\hat{x}$ and $\hat{t}_0$ will equal x and t_0 only if $\hat{v} = v$. The transformation with an approximate velocity, however, will serve as a best guess until an accurate velocity function can be estimated.

A Field Data Example

In this section we show an example of slant stacks applied to field data.

Six simple slant stacks were performed on the data with no provisions made to reduce end effects and aliasing. These practical problems are discussed in the Appendix.

Three numerical values of the ray parameter, p, were chosen for the stack ($p = 0.07, 0.05, 0.03$ msec/ft, giving $\theta = 20.5°, 14.5°$ and $8.6°$ for water velocity). Recall that

$$p = \frac{\sin\theta}{v} = \frac{dt}{df} \tag{2.17}$$

where θ is the propagation angle from the vertical, v is the velocity and (f,t) are the horizontal and vertical coordinates of the common geophone or common shot gather.

The boat direction and the positive x axis are both to the right in all the following sections. Positive values for p, then, imply a wave front traveling down and to the right. Such sections were created from common shot gathers. The negative p sections were created from common geophone gathers.

The sections were transformed to interpretation coordinates before plotting was done. Since we did not have detailed velocity information, we used an approximate water velocity, $v = 5000$ ft/sec, for the transformation. As a result, the sea floor primary reflection and its multiple reflections are properly transformed, but the deeper primaries are not. It would be this transformation that we would use if our purpose was to predict and subtract deep water multiple reflections.

The CMP stacked section which was done by the company which supplied the data is also included. The CMP stack is a summation over hyperbolic trajectories for data in CMP gathers using a best estimate of the subsurface velocities. This section also includes processing which we have not done. For example, we have made no effort to suppress the

multiple sea floor reflections.

We are suggesting that using several p-sections for geologic interpretation can be a useful supplement to a single CMP stacked section. There appear to be some real features of the subsurface reflectors which are apparent in some of the p-sections but not the CMP stack. (These are described individually in the figure captions.) This is not surprising as some reflectors have a highly angle-dependent reflection coefficient. Each p-section is created by illumination from some unique direction, whereas the CMP stacked section is a conglomerate of all available illumination angles.

The signal to noise ratio in a slant stacked section lies somewhere between that of a single offset section and a CMP stacked section. In the CMP stack all events add coherently into the sum, and if we are dealing with a 48 trace gather (as we are with this data), the theoretical signal to noise of the ratio of the stack should be $\sqrt{48}$ times that of each individual trace in the gather. On the other hand, in the slant stacked sections only events inside each Fresnel zone will add coherently into the sum. If four or five Fresnel zones comprise the entire range of propagation angles received by the geophones, then we have a signal to noise ratio of the p-section which is $\sqrt{4}$ or $\sqrt{5}$ times less than that of the CMP. In principle, we expect to be able to recover the signal to noise ratio of the CMP section by summing all of the slant sections together with appropriate moveout corrections.

There are some general features of the p-sections which can be described here:

The wave front in the upper left hand corner of each p-section shows the propagation angle of the downgoing wave in water.

There are a fairly large number of dead traces apparent in the negative p-sections. These are due to shot misfires in the field. Note that they are only readily apparent in positive p-sections because these slant stacks were done over common shot gathers.

There is a region delineated in the left hand side of the p-sections labeled "programming error." This problem affects only that data bracketed.

Reverse Illumination

Throughout this chapter an implication in regard to the slant stack has been that we will always create a plane wave traveling down and toward the geophone in a common geophone gather. Although this is certainly of interest most of the time, situations will arise in which it may be desirable to illuminate the subsurface with a wave traveling away from the geophone, as depicted in Figure 2.21. An obvious case is one in which the desired illumination angle is close to 90 degrees and thus would invite interference from the direct arrival.

The procedure for synthesis by means of the slant plane wave stack is shown in Figure 2.22. Notice that the only difference is a change in the sign of p, the slope of the summation trajectory.

A complication that this procedure introduces is also depicted in Figure 2.22. Unless the data is sampled very densely in the offset dimension, spurious energy from aliasing may contaminate the desired coherent energy from the stack. (See Appendix for an example of aliasing.) This method may only be used, therefore, when spatial sampling is sufficiently dense, and it presents itself as an argument for denser sampling in the field.

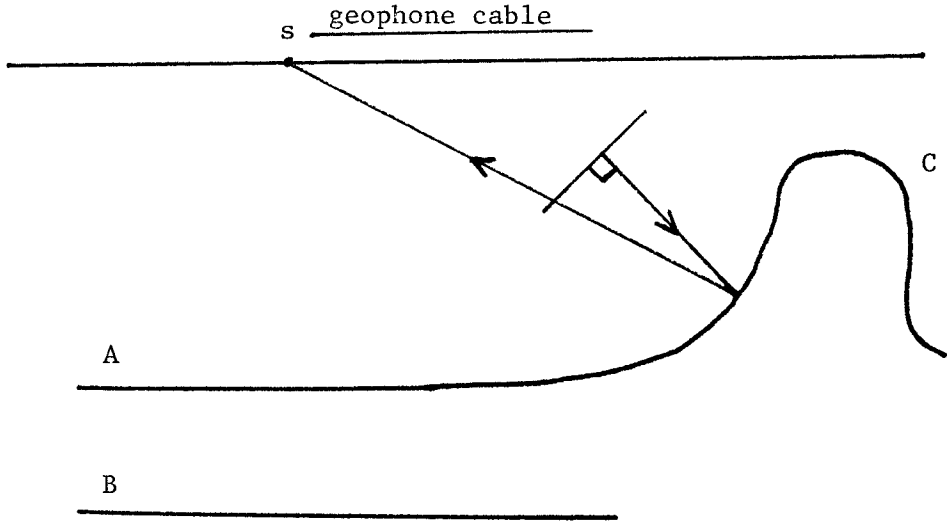

Figure 2.21. In the case of a steeply dipping reflector, we may wish to illuminate it by constructing a plane wave traveling away from the detector. (We have reversed the roles of shot and geophone by reciprocity.) This may be desirable, for example, when the propagation angle of interest is close to 90 degrees and we wish to avoid contaminating energy from the direct arrival.

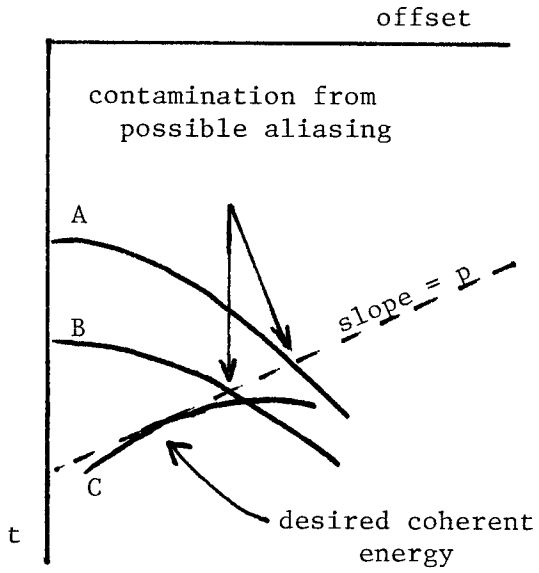

Figure 2.22. The common shot gather from the earth model of Figure 2.21. Our slant summation trajectory has a negative slope to enhance the energy shown in Figure 2.21. Notice that unless the data is sampled very densely, we are in danger of aliasing from events A and B .